O-GlcNAcylation of TDP-43 suppresses proteinopathies and promotes TDP-43's mRNA splicing activity

Meng-Jie Zhao[1,†] (ID), Xiao Yao[2,†], Ping Wei[3,†] (ID), Chen Zhao[2,†], Meng Cheng[2], Dong Zhang[2], Wen Xue[4,5], Wen-Tian He[6], Weili Xue[2], Xinxin Zuo[2], Lei-Lei Jiang[6], Zhiyuan Luo[7], Jiaqi Song[2], Wen-Jie Shu[2] (ID), Han-Ye Yuan[2], Yi Liang[2], Hui Sun[2], Yan Zhou[7], Yu Zhou[2] (ID), Ling Zheng[2] (ID), Hong-Yu Hu[6], Jiwu Wang[4,5,8,*] (ID) & Hai-Ning Du[2,*] (ID)

Abstract

Pathological TDP-43 aggregation is characteristic of several neurodegenerative diseases, including amyotrophic lateral sclerosis (ALS) and frontotemporal lobar degeneration (FTLD-TDP); however, how TDP-43 aggregation and function are regulated remain poorly understood. Here, we show that O-GlcNAc transferase OGT-mediated O-GlcNAcylation of TDP-43 suppresses ALS-associated proteinopathies and promotes TDP-43's splicing function. Biochemical and cell-based assays indicate that OGT's catalytic activity suppresses TDP-43 aggregation and hyperphosphorylation, whereas abolishment of TDP-43 O-GlcNAcylation impairs its RNA splicing activity. We further show that TDP-43 mutations in the O-GlcNAcylation sites improve locomotion defects of larvae and adult flies and extend adult life spans, following TDP-43 overexpression in Drosophila motor neurons. We finally demonstrate that O-GlcNAcylation of TDP-43 promotes proper splicing of many mRNAs, including STMN2, which is required for normal axonal outgrowth and regeneration. Our findings suggest that O-GlcNAcylation might be a target for the treatment of TDP-43-linked pathogenesis.

Introduction

Transactive response DNA-binding protein 43 (TDP-43) is a multifunctional nuclear protein that plays diverse roles in transcription, alternative splicing, RNA stability, and gene regulation (Buratti & Baralle, 2008; Lee *et al*, 2011). TDP-43 pathology is a disease hallmark identified in most amyotrophic lateral sclerosis (ALS) and ~ 50% of frontotemporal lobar degeneration (FTLD) patients (Arai *et al*, 2006; Neumann *et al*, 2006; Ling *et al*, 2013). Mutations in the encoding TDP-43 gene are associated with familial and sporadic ALS and rare cases of FTLD and confer toxicity (Sreedharan *et al*, 2008). While TDP-43 is mainly localized in nucleus, pathological TDP-43 and TDP-43 truncated fragments are primarily found in the cytoplasm with the morphology of abnormal aggregates in the diseased brain and spinal cord (Neumann *et al*, 2006). The cytoplasmic aggregates of TDP-43 in motor neurons could exhibit a toxic gain-of-function with acquirement of abnormal protein–protein and/or protein-RNA interactions, along with defective clearance (Neumann *et al*, 2006; Barmada *et al*, 2010; Kabashi *et al*, 2010). However, a growing body of evidence support that TDP-43 mutations or aggregation induce loss of functions by producing aberrant RNA splicing or sequestering nuclear soluble TDP-43 into cytoplasmic inclusions, thereby loss of splicing and transcription activities (Igaz *et al*, 2011; Polymenidou *et al*, 2011; Arnold *et al*, 2013). Regardless, the mechanism underlying the regulation of TDP-43 function remains poorly understood.

1 Department of Thoracic Surgery, Renmin Hospital of Wuhan University, College of Life Sciences, Wuhan University, Wuhan, China
2 Hubei Key Laboratory of Cell Homeostasis, RNA Institute, College of Life Sciences, Renmin Hospital of Wuhan University, Wuhan University, Wuhan, China
3 Shanghai Diabetes Institute, Shanghai Key Laboratory of Diabetes Mellitus, Shanghai Clinical Center for Diabetes, Shanghai Jiao Tong University Affiliated Sixth People's Hospital, Shanghai, China
4 Clinical Research Institute, Affiliated Nanhua Hospital, University of South China, Hengyang, China
5 Shanghai Institute of Endocrine and Metabolic Diseases, Shanghai, China
6 State Key Laboratory of Molecular Biology, Shanghai Institute of Biochemistry and Cell Biology, Center for Excellence in Molecular Cell Science, Chinese Academy of Sciences, Shanghai, China
7 Frontier Science Center for Immunology and Metabolism, Medical Research Institute at School of Medicine, Wuhan University, Wuhan, China
8 Department of Anatomy and Physiology, Shanghai Jiao Tong University School of Medicine, Shanghai, China
*Corresponding author. Tel: +86 734 8358008; E-mail: jiwu@wang-lab.cn
**Corresponding author. Tel: +86 27 68752401; E-mail: hainingdu@whu.edu.cn
†These authors contributed equally to this work

Post-translational modifications have been extensively studied to be involved in TDP-43 aggregation, stability, and clearance. TDP-43 contains two RNA-recognition motifs (RRMs) participated in DNA or RNA binding, nuclear import and export signals, as well as a C-terminal glycine-rich domain, which harbors the majority of the ALS-linked mutations (Buratti & Baralle, 2001; Pesiridis *et al*, 2009; Cohen *et al*, 2011). Particularly, hyperphosphorylation of S409/S410 sites on TDP-43 is identified as a marker of disease pathology and is commonly found in ALS and FTLD patients, associated with ubiquitinated forms as well as cleaved C-terminal fragments of ~ 35 kDa and ~ 25 kDa (Neumann *et al*, 2006; Zhang *et al*, 2007; Hasegawa *et al*, 2008; Liachko *et al*, 2013; Choksi *et al*, 2014). Phosphorylation of S409/S410 sites might enhance the half-life of TDP-43 and inhibit the proteasome system-mediated degradation, contributing to the formation of aggregates (Zhang *et al*, 2009). Recently, Cohen *et al* (2015) identified that TDP-43 can be acetylated within the RRM domains upon oxidative stress conditions, which results in the loss of function of TDP-43 binding RNA and promotes accumulation of the TDP-43 aggregates in cultured cells. These findings highlight a new pathological mechanism underlying the regulation of post-translational modifications of TDP-43.

O-GlcNAcylation, a type of protein O-glycosylation by which the monosaccharide N-acetylglucosamine (GlcNAc) attached to Ser/Thr residues via an O-linked glycosidic bond, has been reported to regulate diverse cellular metabolisms and involved in neurodegenerative diseases (Khidekel *et al*, 2007; Yuzwa & Vocadlo, 2014). In vertebrate, O-GlcNAcylation is added to proteins by a sole enzyme, named as OGT (O-linked N-acetylglucosamine transferase) and removed it from proteins by a sole enzyme, termed OGA (O-GlcNAcase) (Slawson & Hart, 2011). One of well-known examples related to neurodegenerative diseases is tau O-GlcNAcylation, which extensively occurs in bovine and human brains (Arnold *et al*, 1996; Liu *et al*, 2004). Increasing O-GlcNAc levels can block phosphorylation of tau and attenuate the formation of tau aggregates, common pathological features of tau-associated neurodegenerative disorders (Lefebvre *et al*, 2003; Yuzwa *et al*, 2008; Yuzwa *et al*, 2012). Since hyperphosphorylation and abnormal aggregation of TDP-43 are implicated in ALS and FTLD, we hypothesize that TDP-43 is able to be O-GlcNAcylated, which regulates TDP-43-related proteinopathies and functions.

Results

TDP-43 can be O-GlcNAcylated by OGT *in vivo*

To test our hypothesis, we first examined whether TDP-43 is O-GlcNAcylated. Thus, endogenous TDP-43 was immunoprecipitated from the human SH-SY5Y neuroblastoma cells, and the O-GlcNAcylation of TDP-43 was detected (Fig 1A). Alternatively, immunoprecipitation assays were performed using a specific O-GlcNAcylation recognition antibody, and the O-GlcNAcylated TDP-43 was also detected by immunoblotting (Fig 1B). To verify the specificity of the detected O-GlcNAcylated species, we applied thiamet-G (TMG) and PUGNAc, inhibitors of OGA, and OSMI-1, an inhibitor of OGT, to treat HEK 293T cells expressing GFP-tagged TDP-43 (Fig 1C) or Flag-tagged TDP-43 (Fig 1D). As expected, inhibition of OGA increased O-GlcNAc levels of exogenous TDP-43, whereas inhibition

of OGT decreased its O-GlcNAc level (Fig 1C and D). The global O-GlcNAc levels of cell lysates served as a detection control. Consistently, the O-GlcNAcylation levels of TDP-43 were gradually increased when cells treated with different amounts of uridine diphosphate-N-acetylglucosamine (UDP-GlcNAc), a biochemical precursor of synthesizing glycosylated proteins, in a dose-dependent manner (Fig 1E and F). In addition, overexpression of wild-type (WT) OGT, but not the catalytic-inactive mutant of OGT (H498N), substantially increased the O-GlcNAcylated level of TDP-43 (Fig 1G and H). Conversely, overexpression of the WT OGA, but not the catalytic-inactive mutant of OGA (D174/175N), significantly decreased the O-GlcNAcylated level of TDP-43 (Fig 1I and J). To determine the extent of O-GlcNAcylated TDP-43 in cellular context, cells were treated with TMG with different times, and the global O-GlcNAcylation levels of cellular proteins were compared (Fig EV1A). We noticed that the O-GlcNAcylation levels remain constant since 12 h treatment. Thus, we supposed the O-GlcNAcylation extent of TDP-43 with 48-h treatment as 100%, and the relative O-GlcNAcylation levels of TDP-43 in untreated cells were compared and quantified with the signal intensity in treated cells. It turns out that ~ 20% TDP-43 was modified with O-GlcNAcylation, suggesting the importance of this modification (Fig EV1B and C). Of note, the inhibitor of OGA could not completely block the removal of O-GlcNAc moieties, the modified percentage of TDP-43 by OGT was most likely less than we examined above. Nevertheless, we certainly can draw a conclusion that TDP-43 is O-GlcNAcylated by OGT *in vivo*.

OGT suppresses TDP-43-induced cellular toxicity and aggregate formation

We wondered if OGT affects TDP-43-associated proteinopathies. Thus, a well-established yeast TDP-43 system was used to recapitulate some salient features of human TDP-43 (hTDP-43) proteinopathies, including cellular toxicity and protein aggregation (Johnson *et al*, 2008). In line with previous studies, galactose-inducible high levels of hTDP-43 in yeast cells led to dramatic inhibition of growth compared with cells transformed with empty vectors with epitopic tag alone (Fig 2A, row 2 vs. row 1). Strikingly, co-expression of OGT in yeast predominantly alleviated the suppression of cell growth caused by TDP-43 overexpression. This impact is dependent on the enzymatic activity of OGT, as co-expression of the catalytic-inactive mutant of OGT could not comparably recue the slow growth defects (Fig 2A, row 3 vs. 4). Of note, constitutive overexpression of OGT in the absence of TDP-43 (lacking galactose induction) would not affect cell toxicity (Fig 2A, left panel, row 3 vs 1). Intriguingly, co-expression of OGT with ALS-linked Q331K mutant of TDP-43 also compromised the growth defect, suggesting the potential implication of OGT in preventing TDP-43-associated proteinopathy (Fig 2A, row 6 vs. 5). The compromised growth defects by OGT overexpression did not result from dramatic reduction of TDP-43 levels, but from reduced TDP-43 aggregates in cells (Fig 2B and C). Quantitation analysis showed that the cell population containing > 3 GFP foci were markedly decreased upon overexpression of WT OGT, but not catalytic inactive mutant (Fig 2D). Therefore, the results indicated the role of OGT in suppression of cellular toxicity and inhibition of TDP-43 aggregation.

OGT represses TDP-43 hyperphosphorylation and insoluble pellet formation

Next, we test if OGT could relieve TDP-43 proteinopathy by preventing TDP-43 hyperphosphorylation. Indeed, cells treated with GlcNAc, increased O-GlcNAcylation level of TDP-43, accompanied with decreased phosphorylation level of TDP-43 (Fig 3A and B). Consistent with previous results, cells treated with ethacrynic acid (EA) resulted in an increase of phosphorylation levels (Iguchi et al, 2012), whereas we also observed a significant decrease of O-

GlcNAcylation levels of TDP-43, examined by Western blotting and immunofluorescence staining (Fig 3C–E). By contrast, when cells were treated with a combination of GlcNAc and EA, the phosphorylation levels of TDP-43 dropped down to a comparable level of mock-treated cells, accompanied with a recovery of O-GlcNAc levels of TDP-43 (Fig 3C). Accordingly, immunofluorescence analysis showed an increased cell population with positively staining with phosphorylated TDP-43 in EA-treated cells, but not in cells treated with either GlcNAc only or a combination of EA and GlcNAc (Fig 3D and E). Furthermore, solubility assays showed that
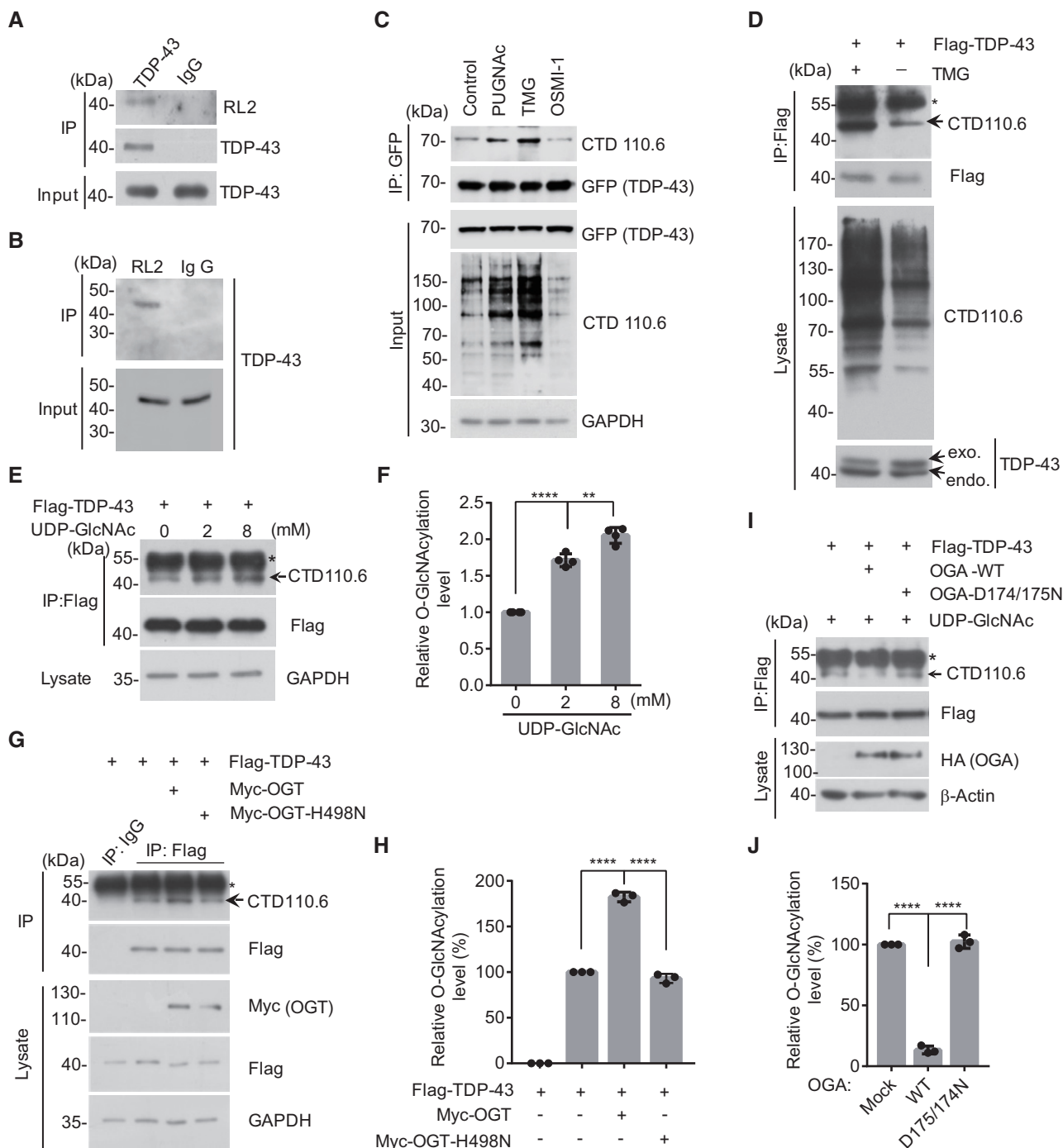

Figure 1.

Figure 1. TDP-43 is O-GlcNAcylated by OGT in mammalian cells.

A O-GlcNAcylation signals of TDP-43 were examined by immunoblotting with immunoprecipitated TDP-43 from SH-SY5Y cells. IgG immunoprecipitation served as a negative control.
B The O-GlcNAcylated TDP-43 was immunoprecipitated by the RL2 antibody and examined by immunoblotting against a TDP-43 antibody.
C HEK 293T cells were treated with the indicated compounds for 36 h, and the O-GlcNAc levels of TDP-43 were examined.
D SH-SY5Y cells expressing Flag-TDP-43 constructs were treated with TMG, and the O-GlcNAc levels of TDP-43 were examined. Endogenous (endo.) and exogenous (exo.) TDP-43 were indicated.
E Cells overexpressing Flag-TDP-43 were treated with increasing doses of UDP-GlcNAc, and the O-GlcNAcylation levels of TDP-43 were detected.
F Quantification of (E). Mean ± SD, unpaired two-tailed *t*-test, *n* = 4 biological replicates.
G Overexpression of WT OGT, but not catalytic-inactive OGT mutant, increased the O-GlcNAc levels of TDP-43. OGT protein levels were examined by immunoblotting.
H Quantification of (G). Mean ± SD, unpaired two-tailed *t*-test, *n* = 3 biological replicates.
I Overexpression of WT OGA, but not catalytic-inactive OGA mutant, abated the O-GlcNAc levels of TDP-43. OGA protein levels were examined by immunoblotting.
J Quantification of (G). Mean ± SD, unpaired two-tailed *t*-test, *n* = 3 biological replicates.

Data information: The black arrows in different panels indicate O-GlcNAcylated TDP-43 bands; the asterisks in different panels indicate heavy-chain bands. $**P < 0.01$, $****P < 10^{-4}$.
Source data are available online for this figure.

overexpression of the WT OGT, but not the catalytic-inactive mutant, apparently reduced the SDS-insoluble fractions of endogenous TDP-43 (Fig 3F and G, lane 2 vs. 3), but less significant in the presence of EA (Fig 3F and G, lane 5 vs. lane 6). The results indicated that OGT may only play a minor role in suppression of TDP-43 aggregation under stress conditions, and alternative indirect mechanisms may operative that protect cells against TDP-43-associated proteinopathies. Interestingly, overexpression of OGT was also capable of preventing EA-induced TDP-43 fragmentation (35 kDa and 25 kDa) detected in the SDS-insoluble fraction (Fig 3H, lane 5 vs. lane 6), which is also a disease hallmark of TDP-43 proteinopathy. Quantitative analysis showed that insoluble moieties of the full-length TDP-43 increased with EA treatment, whereas reduced upon OGT expression (Fig 3I). Collectively, these data imply that OGT-mediated O-GlcNAcylation of TDP-43 represses TDP-43-associated pathology.

OGT directly O-GlcNAcylates TDP-43 primarily at the T199 and T233 sites

We next investigate whether OGT modify TDP-43. We first confirmed that endogenous TDP-43 can co-immunoprecipitate with OGT in SH-SY5Y cells (Fig 4A). *In vitro* O-GlcNAcylation assay showed that OGT directly GlcNAcylated recombinant TDP-43 (Fig 4B). Next, the potential OGT-modified sites on TDP-43 are identified. HEK 293T cells expressing Flag-TDP-43 in the presence of GlcNAc were immunoprecipitated with α-Flag resins, and enriched TDP-43 elutes were subjected to mass spectrometry (MS) analysis. The MS data showed that threonine 199 (T199), serine 212 (S212), and threonine 233 (T233) residues were the candidate glycosylation sites of TDP-43 (Fig EV2A and B). Noticeably, T199 and T233 are conserved in higher eukaryotic organisms, and both sites are located at the second RRM domain (RRM2) (Fig 4C). The solved structure of TDP-43 showed that both sites in RRM2 domain do not directly interact with nucleic acids, indicating that mutations of these residues may not influence the high-order structure of TDP-43 (Fig 4D). To determine whether these two conserved residues represent the major O-GlcNAcylated sites in TDP-43, T199A, T233A, and T199A/T233A double mutant (2TA) were generated, and the O-GlcNAcylation levels of TDP-43 were examined. Given that bacterial expression of the full-length TDP-43 is insoluble, GST-tagged TDP-43 fragments (a.a. 102-269) bearing the two O-GlcNAcylation sites

were constructed. Immunopurified Flag-tagged OGT from HEK 293T cells was incubated with various recombinant GST-TDP-43 fragments in the presence of the donor of UDP-GlcNAc. The *in vitro* assay showed that the T199A or T233A mutant exhibited reduced O-GlcNAcylation signals, whereas the 2TA mutant abolished O-GlcNAcylation signal (Fig 4E and F). Moreover, we found that the O-GlcNAcylation level of exogenous expressed T199A or T233A mutant of GFP-tagged TDP-43 was obviously reduced, while that of the 2TA mutant barely detected compared with the WT (Fig 4G and H). Of note, S212A mutation of TDP-43, which is also located in the RRM2, did not markedly affect its O-GlcNAcylation level, suggesting the importance of the other two conserved O-GlcNAcylation sites (Fig 4G). Interestingly, the O-GlcNAc level of ALS-linked Q331K mutant did not evidently change, suggesting other unknown mechanism involved in ALS pathogenesis (Fig EV3). Altogether, these results indicate T199 and T233 are the main O-GlcNAcylation sites of TDP-43.

O-GlcNAcylation of TDP-43 affects locomotion and longevity of *Drosophila*

Drosophila melanogaster has been widely used as a powerful tool for studying neurodegenerative diseases, including ALS (Bilen & Bonini, 2005; Li *et al*, 2010). It has been shown that overexpression of either hTDP-43 or the fly homolog of TDP-43 (TBPH) in *Drosophila* recapitulates several ALS features, such as neuronal loss, life span shorten, and locomotor dysfunction (Estes *et al*, 2011; Wang *et al*, 2011). Thus, we decided to utilize *Drosophila* as a model to study the effect of O-GlcNAcylation of TDP-43 in ALS features. hTDP-43 or its O-GlcNAcylation-deficient mutants were specifically expressed in motor neurons using a neuronal expression (C155-GAL4) system, and locomotor behavior was examined by quantitative video tracking of either larval crawling speed or adult fly climbing speed (Fig 5A–C). Consistently, the locomotive ability of overexpressing WT hTDP-43 was remarkably impaired at both late third instar larvae (62.2% decrease, $P < 0.0001$) and adult stages (0.09 cm/s vs. 2.15 cm/s) relative to the control, indicative of TDP-43-dependent dysfunction (Fig 5A–C). In addition, the majority of WT-overexpressed adult flies were unable to fly, walked slowly, and fell over frequently (Movie EV1 and 2). In contrast, overexpression of any O-GlcNAcylation-deficient mutants of hTDP-43, with different extent, rescued slow locomotive defects compared with WT
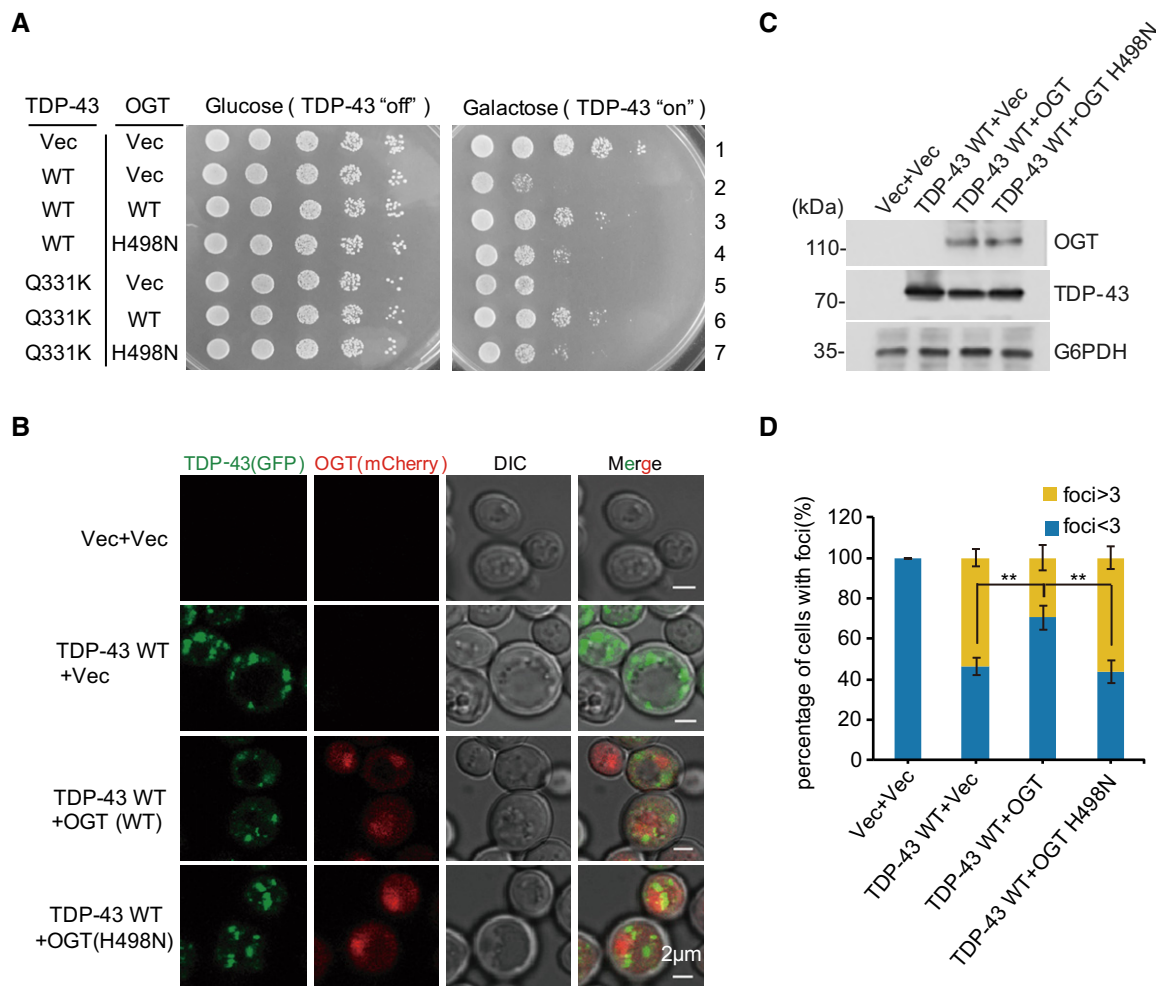
Figure 2. OGT suppresses TDP-43-induced cellular toxicity and protein aggregation in budding yeast.

A Yeast cells that express galactose-inducible GFP-tagged hTDP-43 only or co-expressing mCherry-tagged WT or catalytic-inactive mutant of OGT, were spotted onto plates containing glucose or galactose. Cell growth was assessed after 2 days.

B Yeast cells expressing the indicated constructs were induced in galactose-containing medium, and representative images were shown using fluorescence microscopy to visualize TDP-43 aggregates. DIC: Differential interference contrast. Scale bar: 2 μm.

C Expression levels of TDP-43 in strains of (B) were examined by immunoblotting.

D TDP-43 aggregate foci numbers from individual cell of (B) were quantified from over 50 cells each of the indicated yeast strains. The foci numbers in individual cell > 3 were labeled with yellow, and the foci numbers in individual cell < 3 are labeled with blue. Mean ± SD, unpaired two-tailed *t*-test, *n* = 3 for each samples, biological replicates. **$P < 0.01$.

Source data are available online for this figure.

overexpression, suggesting that they partially compromised the toxicity of WT TDP-43 (Fig 5A–C, and Movie EV3-5). Noticeably, we observed that the 2TA mutant completely restored the larval crawling ability ($P > 0.85$), but still exhibited slower adult locomotor speed (1.49 cm/s vs. 2.15 cm/s, $P = 0.0002$), when compared to the control, which suggests that the 2TA mutant possesses neuronal toxicity in adult flies (Fig. 5C). The divergent phenotypes did not result from different expression levels of TDP-43, but probably from different O-GlcNAc levels, implying the role of this modification on TDP-43 (Fig 5D).

A recent study indicated that high glucose diet can improve locomotion and life span defects caused by TDP-43 overexpression in motor neurons (Manzo *et al*, 2019). Therefore, we fed the hTDP-43 expressing flies either a regular (4% sucrose) or high sugar (16%

sucrose) diet. Since sucrose can be broken down to form glucose and directly enter the hexosamine biosynthesis pathway and serve as the substrate for O-GlcNAc, we assumed that higher sucrose diet can improve the fly locomotor dysfunction, likely similar to the previous phenotype shown in larval turning assays (Manzo *et al*, 2019). Indeed, we observed that high sucrose diet alleviated the adult locomotive deficit caused by neuronal expression of WT hTDP-43 (Movie EV6). In addition, overexpression of WT, T199A, or T233A hTDP-43, but not of the 2TA mutant, in neurons significantly reduced fly life spans compared with that in control flies, suggestive of their higher neuronal toxicity (Fig 5E). Interestingly, we observed that high sucrose diet apparently extended fly life spans, to a certain extent, in the WT, T199A, or T233A hTDP-43
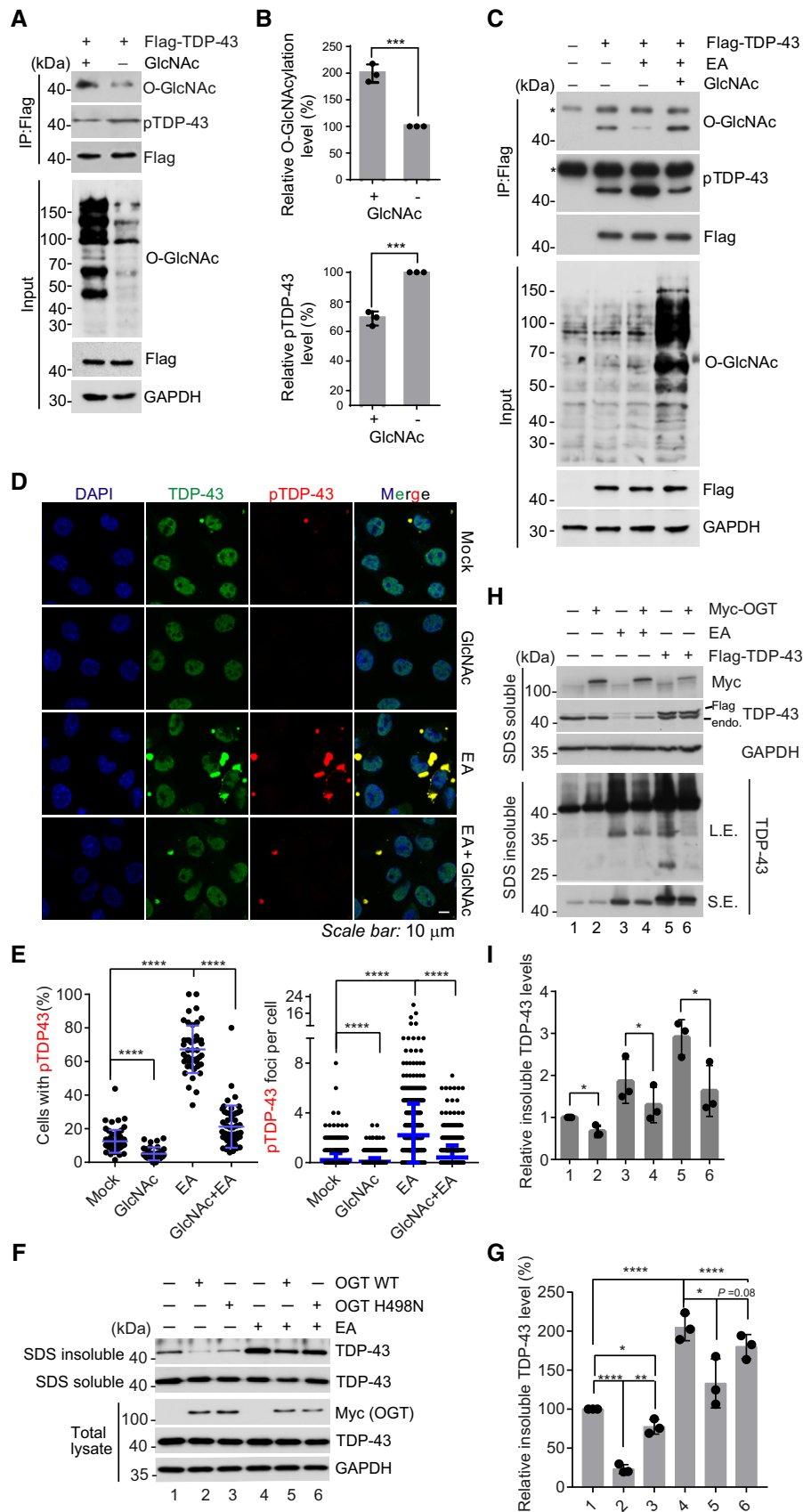
Figure 3.

◀

Figure 3.   OGT suppresses TDP-43-associated proteinopathies in mammalian cells.

A   SH-SY5Y cells overexpressing Flag-TDP-43 were treated with GlcNAc, and the O-GlcNAcylated and phosphorylated (pTDP-43) levels of TDP-43 were examined by immunoblotting.

B   Relative O-GlcNAcylation levels (top) and phosphorylation levels (bottom) of TDP-43 shown in (A) were quantified. Mean ± SD, unpaired two-tailed *t*-test, *n* = 3 biological replicates.

C   SH-SY5Y cells overexpressing Flag-TDP-43 were treated with either 20 μM EA or 2 mM GlcNAc or a combination. The O-GlcNAcylated or phosphorylated levels of TDP-43 were examined by immunoblotting. The asterisks indicate heavy-chain bands.

D   SH-SY5Y cells treated with the indicated compounds were immunostained with TDP-43 or pTDP-43 and observed by immunofluorescence. Scale bar: 10 μm.

E   Quantification of signal intensities of pTDP-43 staining (left) or foci numbers per cell (right). Cell number counted: left panel, "Mock" *n* = 58, "GlcNAc" *n* = 35, "EA" *n* = 45, "GlcNAc + EA" *n* = 52; right panel, "Mock" *n* = 1167, "GlcNAc" *n* = 1051, "EA" *n* = 542, "GlcNAc + EA" *n* = 815. Mean ± SD, unpaired two-tailed *t*-test.

F   SDS-soluble and insoluble fractions were isolated from SH-SY5Y cells expressing WT or catalytic-inactive mutant OGT treated with 20 μM EA, and the fractions were analyzed by immunoblotting.

G   Quantification of (F). Mean ± SD, unpaired two-tailed *t*-test, *n* = 3 biological replicates.

H   SDS-soluble and insoluble fractions were isolated from SH-SY5Y cells expressing WT OGT and/or Flag-TDP-43 in the presence or absence of EA, and the truncated TDP-43 fragments were examined by immunoblotting. L.E.: long exposure; S.E.: short exposure.

I   Quantification of (H). Mean ± SD, unpaired two-tailed *t*-test, *n* = 3 biological replicates.

Data information: *$P < 0.05$, ***$P < 0.001$, ****$P < 10^{-4}$.
Source data are available online for this figure.

overexpressed flies. Specifically, the average life span of WT expressed flies fed with regular sucrose diet was 10 days, with a 60% increase of life span fed with high sucrose diet (16 days). The life spans of T199A and T233A expressed flies were longer than that of WT, and their average life spans increased 13% or 3.7% after fed with high sucrose diet, respectively. Of note, flies expressing the 2TA mutant of TDP-43 showed no difference of life span even fed a higher sugar diet, suggesting the importance of O-GlcNAcylation occurred on these two sites (Fig 5E). The difference of life span in the same fly strain fed with different sugar diets apparently did not result from the impact of protein expression, as the similar hTDP-43 protein levels in each pair of samples were detected (Fig 5F).

Next, we want to validate whether the alleviated ALS features in these indicated TDP-43 overexpressed larvae or adult flies upon high sugar availability come from O-GlcNAcylated modification on these two sites. Thus, hTDP-43 and OGT were co-expressed in motor neurons, which alleviated the locomotor deficits compared to hTDP-43 expression alone (Fig 5G and H). In contrast, co-expression of OGT and the 2TA mutant could not further enhance its locomotor deficits compared to hTDP-43 expression alone (Fig 5I and J). We also observed that expression of OGT alone decreased locomotor ability of adults, which might result from OGT-mediated other functions. It should point out that a catalytic activity-independent role of OGT might be involved, and further investigation would be useful to answer this question. Regardless, these results suggest that O-GlcNAcylation of hTDP-43 by OGT can partly relieve those phenotypes including locomotor deficits and shorter life span in *Drosophila*, and the two identified O-GlcNAcylation sites are important to relieve ALS-linked neurodegeneration.

O-GlcNAcylation of TDP-43 regulates mRNA splicing

Regulation of alternative splicing is one of the most important functions of TDP-43. High-throughput sequencing approaches have shown that downregulation of TDP-43 in mouse brain led to distinct splicing alternations of mRNAs (Polymenidou *et al*, 2011; Tollervey *et al*, 2011). To test whether O-GlcNAcylation regulates mRNA splicing function of TDP-43, a cell-based nuclear CFTR (cystic fibrosis transmembrane conductance regulator) splicing assay was performed (Buratti *et al*, 2001; Che *et al*, 2011). We employed a previously reported TDP-43-specific siRNA

(Tollervey *et al*, 2011), which significantly reduced endogenous TDP-43 levels, without interfering with expression of co-transfected RNAi-resistant WT or other indicated TDP-43 mutants (Fig 6A). As expected, TDP-43 knockdown resulted in the accumulation of the exon 9 unspliced transcript and a marked reduction in the spliced/unspliced ratio, while adding back WT TDP-43 rescued this phenotype by enhancing the spliced/unspliced ratio, compared to the control. However, the 2TA, but not T199A or T233A mutant, lost the mini-CFTR alternative splicing ability, suggesting the importance of O-GlcNAcylation on these sites (Fig 6A). We confirmed that loss of RNA splicing abilities in these O-GlcNAc defective mutants did not result from the loss of RNA-binding abilities using the RNA electrophoretic mobility shift assay (RNA-EMSA). We found that the interactions of the WT or mutants of TDP-43 with biotinylated synthetic RNA sequence of IL-6 intron 2 are equivalent (Fig EV4). By contrast, the RNA-binding-deficient 4FL mutant also lost its splicing activity, whereas ALS-linked Q331K mutant still retained, which is accordance with previous reports (Fig 6A) (Daigle *et al*, 2013).

To directly link the influence of OGT on RNA splicing with O-GlcNAcylation of TDP-43 but not other substrates, two combined experiments were performed. First, knockdown of OGT itself was sufficient to attenuate TDP-43-dependent CFTR exon 9 splicing, and double knockdown of OGT and TDP-43 displayed a comparable splicing signal with that by knockdown of TDP-43 alone, suggesting the relation of OGT to TDP-43 on CFTR splicing (Fig 6B). Furthermore, we found that only overexpression of WT OGT, but not the catalytic-inactive mutant of OGT, promoted CFTR exon 9 spliced, implying a potential role of O-GlcNAcylation (Fig 6C, lane 1–3). We also observed that, in the absence of TDP-43, overexpression of OGT failed to promote CFTR splicing (Fig 6C, lane 4 vs. 5). Introduction of WT TDP-43 but not O-GlcNAc-defective 2TA mutant into siTDP-43 cells was able to rescue CFTR splicing ability, which indicates that the effect of OGT on CFTR splicing mainly relies on TDP-43, but not other substrates (Fig 6C, lane 7–12). The unchanged splicing levels upon overexpression of OGT are probably due to the existence of endogenous OGT (Fig 6C, lane 7–9).

It is known that *OGT* genes are highly conserved in all metazoans but has multiple splice variants, but how those variants are generated has poorly investigated (Slawson & Hart, 2011). Based on previous CLIP-Seq dataset, we found that that TDP-43 displayed a stronger binding at several intron regions, but was only proven to silence exon 7 expression as described previously (Fig EV5A)
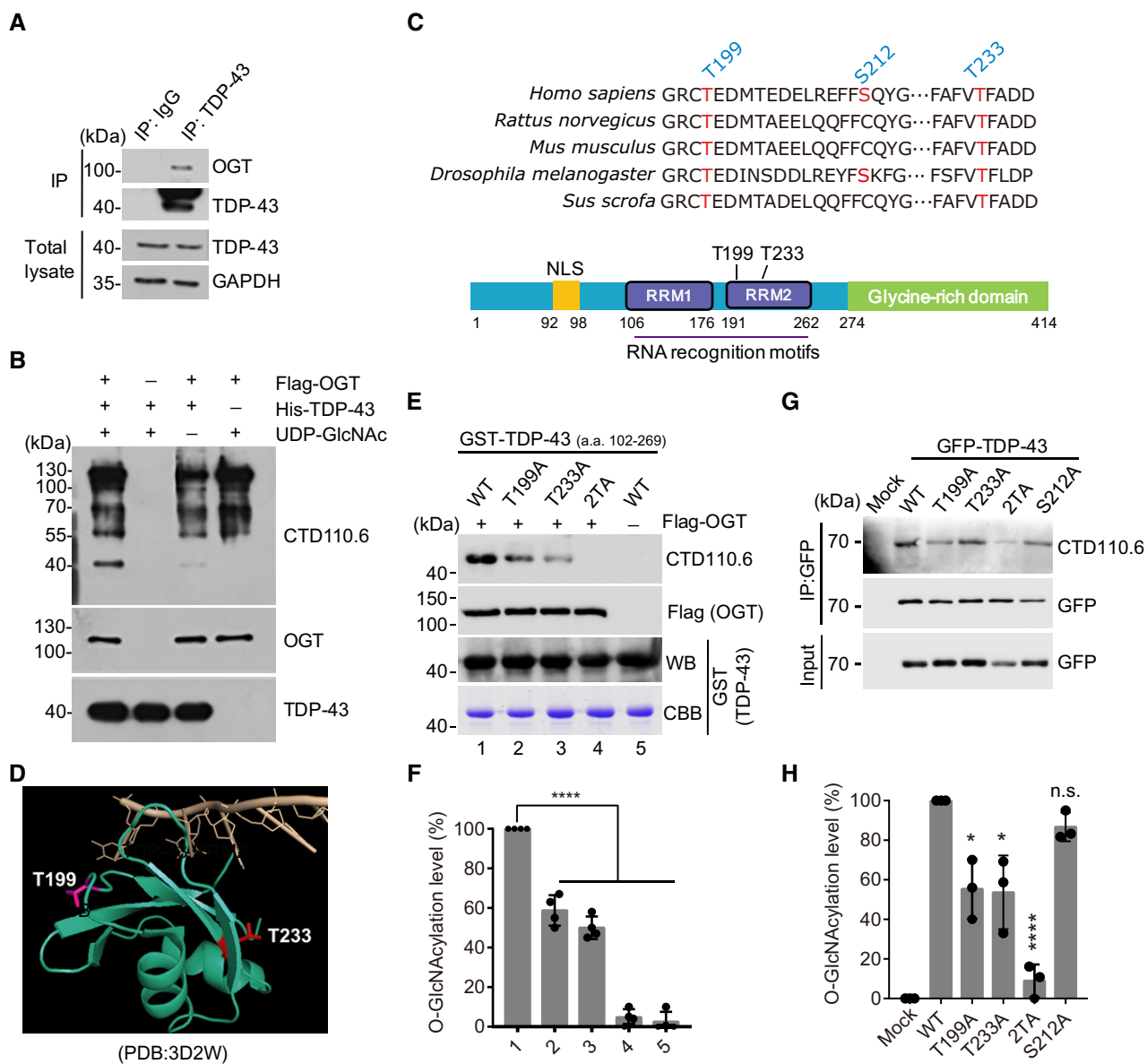
Figure 4. Identification of O-GlcNAcylation sites of TDP-43.

A TDP-43 interacts with OGT examined by immunoblotting.

B *In vitro* glycosylation assay was performed using immunoprecipitated OGT incubated with recombinant His-tagged TDP-43 in the presence of UDP-GlcNAc. The O-GlcNAcylated TDP-43 protein was detected by immunoblotting.

C Sequence alignment of TDP-43 segments containing the identified O-GlcNAcylation sites in different species. The amino acids with red color display the conserved O-GlcNAcylated sites.

D Structural modeling of the RRM2 domain bound to a single strand DNA illustrates the O-GlcNAcylation sites T199 (pink) and T233 (red) of TDP-43 with surrounded DNA (light orange).

E *In vitro* glycosylation assays were performed using immunoprecipitated Flag-OGT incubated with recombinant GST-tagged TDP-43 fragments (a.a. 102-269) in the presence of UDP-GlcNAc. The O-GlcNAcylated TDP-43 proteins were detected by immunoblotting.

F Quantification of (E). Mean ± SD, unpaired two-tailed *t*-test, $n = 4$ biological replicates. $****P < 10^{-4}$.

G Cells expressing the indicated forms of GFP-TDP-43 were subjected to immunoprecipitation, and the O-GlcNAcylated levels of TDP-43 were examined.

H Quantification of (G). Mean ± SD, unpaired two-tailed *t*-test, $n = 3$ biological replicates. $*P < 0.05$, $****P < 10^{-4}$, n.s. not significant.

Source data are available online for this figure.

(Tollervey *et al*, 2011). To test whether O-GlcNAcylation of TDP-43 is necessary for *OGT* mRNA splicing, various Flag-TDP-43 constructs were individually expressed in HEK 293T cells and pre-mRNA splicing events were assessed by PCR analysis. We found that overexpression of WT TDP-43 promoted exclusion of exon 7 of *OGT*. In addition, the O-GlcNAcylation-deficient T199A and T233A mutants displayed a partial reduction in the spliced/un-spliced ratio, while exon 7 exclusion was entirely abolished in the

2TA, Q331K, and 4FL mutants, relative to the control (Fig EV5B). These results indicate that the nuclear factor TDP-43 may participate in *OGT* splicing.

Since TDP-43 targets multiple RNAs that are essential for proper neuronal development and synaptic function, we analyzed the ability of the O-GlcNAcylation-deficient TDP-43 mutants in regulating mRNA splicing of several known target genes in mouse Neuro-2a cells (Tollervey *et al*, 2011). Consistently, overexpression of WT TDP-43 or Q331K mutant resulted in more exclusion of the exons in *Dnajc5* (DnaJ homolog subfamily C member 5) and *Sort1* (Sortilin
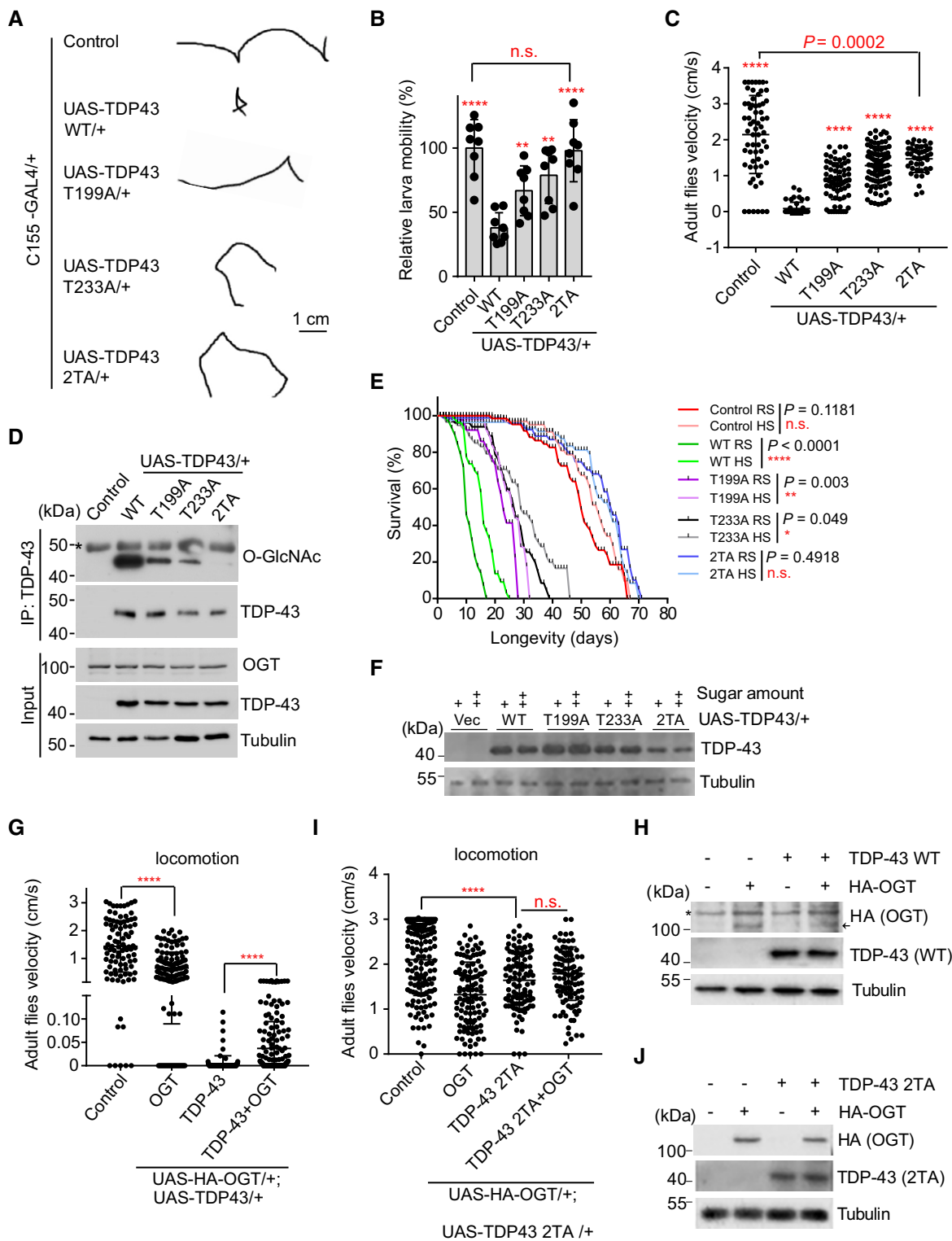

Figure 5.

1). However, the O-GlcNAcylation-deficient mutants exhibited a reduced exclusion of the exons in these transcripts (Fig 6D and E). In addition, rescue experiments showed that the splicing defects induced by knockdown of endogenous TDP-43 could be restored by expressing WT hTDP-43 and the T199A mutant, but not by the T233A and 2TA mutants, which indicates that O-GlcNAcylation of TDP-43 is required for functioning in mRNA splicing (Fig 6F and G).

More recently, Cleveland and Eggan groups identified that STMN2 (a neuronal growth-associated factor Stathmin-2) is necessary for normal axonal outgrowth and regeneration, which is regulated by TDP-43. Reduced nuclear TDP-43 levels link with aberrant production of a spliced exon (called exon 2a) and decreased expression of *STMN2*, which may be as a disease hallmark of TDP-43-dependent ALS patients (Klim *et al*, 2019; Melamed *et al*, 2019). To test whether O-GlcNAcylation of TDP-43 could affect *STMN2*, endogenous TDP-43 was knockdown and various TDP-43 mutants were co-expressed in SH-SY5Y cells, and expression of exon-2a was examined by PCR. Consistently, reduction of TDP-43 induced exon 2a production. Expression of WT TDP-43, as well as the T199A and Q331K mutants, in the TDP-43 depletion cells compromised exon 2a expression. By contrast, expression of the T233A or 2TA mutants still exhibited exon 2a products (Fig 6H and I). As expected, knockdown of endogenous TDP-43 remarkably reduced *STMN2* expression levels, but co-expression of WT, T199A or T233A mutants rescued its levels (Fig 6J). Strikingly, co-expression of 2TA mutant could not enhance *STMN2* levels, emphasizing the importance of O-GlcNAcylation of TDP-43 on mRNA splicing. Taken together, these results indicate that O-GlcNAcylation of TDP-43 is required for proper mRNA splicing, thereby functioning in neurite growth and axon regeneration.

Discussion

In this study, we have provided both *in vitro* and *in vivo* evidence that TDP-43 can be O-GlcNAcylated, which is a novel modification occurred on TDP-43 and that positively regulates its RNA splicing function and suppresses TDP-43-associated proteinopathies. Upregulation of OGT activities would attenuate many of the pathological hallmarks including protein aggregation, cellular toxicity, and hyperphosphorylation. Mechanistically, TDP-43 is primarily O-

GlcNAcylated at the T199 and T233 sites by OGT. Abolishment of O-GlcNAcylation results in its loss of the toxicity in locomotor deficit and the shorter life spans caused by overexpression of hTDP-43 in *Drosophila*, which likely comes from its altered splicing activity. Indeed, mutations in the O-GlcNAcylation of TDP-43 compromise, to different extent, its alternative splicing function, particularly affecting proper splicing of a microtubule regulator-coding gene *STMN2*, which may lead to TDP-43-linked neurodegeneration. Overall, using yeast, cultured neuron cells, and *Drosophila* models, we provide strong evidence that O-GlcNAcylation of TDP-43 is critical for RNA splicing function as well as blocking TDP-43 pathogenesis.

Regulation of alternative splicing is one of the most important functions of TDP-43. CLIP-Seq data in the previous study indicated that TDP-43 showed a stronger binding at the intron regions between exon 3 and exon 4, as well as exon 6 and exon 7 of *OGT* transcript (Tollervey *et al*, 2011). Based on previous study that exon 7 was silenced by OGT, we confirmed that TDP-43 is capable of regulating exon 7 splicing of *OGT*. It is known that *OGT* genes are highly conserved in all metazoans but has multiple splice variants, but how those variants are generated has poorly investigated. Our results pinpoint that one type of *OGT* spliced forms may be mediated by TDP-43. In turn, disruption of TDP-43 O-GlcNAcylation by mutating the two modified sites compromised the pre-mRNA splicing of multiple genes, which exhibits a new role of O-GlcNAcylation beyond modulating signaling, transcription, and cytoskeletal functions (Slawson & Hart, 2011).

The abundance of O-GlcNAc is sensitive to glucose availability. One hallmark of Alzheimer's disease is the impaired glucose uptake and metabolism in patient brains, which has been demonstrated to be a cause, rather than a consequence, of neurodegeneration (Heiss *et al*, 1991; Hoyer, 2004). Agreed with these, glycolysis upregulation can also improve locomotor and life span defects caused by TDP-43 proteinopathy in ALS-linked *Drosophila* model, in which glucose uptake pathway is activated and may protect neuron degeneration (Manzo *et al*, 2019). However, a line of evidence also suggests that O-GlcNAcylation of the key regulatory factors, such as tau protein, is critical for protecting tauopathies and extending longevity in mouse model. For instance, starvation would reduce O-GlcNAcylation levels and consequent hyperphosphorylation of tau in the mouse brains (Liu *et al*, 2004). In addition, it has been found that O-GlcNAcylation of tau is reduced accompanied with abnormal

Figure 6.

◀

Figure 6. TDP-43 O-GlcNAcylation regulates mRNA splicing.

A CFTR splicing assay was examined in cells expressing various TDP-43 constructs by PCR analysis. The numbers represented the relative ratios of exon 9 exclusion (−) vs. inclusion (+) (top panel). Both endogenous (endo.) and exogenous (exo.) TDP-43 protein levels in the indicated samples were examined by immunoblotting (bottom panel).

B CFTR splicing assay was performed in cells with knockdown of either OGT, TDP-43, or combination. *ACTB* levels served as loading controls (top panel). The indicated protein levels were examined by immunoblotting (bottom panel).

C CFTR splicing assay was examined in siTDP-43 cells overexpressing the WT or mutant OGT by PCR analysis. *ACTB* levels served as loading controls (top panel). Various protein levels were examined by immunoblotting (bottom panel).

D Representative gel images for alternative exons in *Dnajc5* and *Sort1* genes in Neuro 2a cells expressing the indicated Flag-TDP-43 constructs were shown (top panel). TDP-43 protein levels were examined by immunoblotting (bottom panel).

E The relative ratios of exclusion to inclusion (−/+) were quantified. Mean ± SD, unpaired two-tailed *t*-test, *n* = 3 biological replicates.

F Neuro-2a cells expressing doxycycline-inducible shRNA knockdown of TDP-43 were transfected with the indicated TDP-43 constructs, and the alternative exons in *Dnajc5* and *Sort1* genes were examined by PCR. Representative gel images were shown (top panel). TDP-43 protein levels were examined by immunoblotting (bottom panel).

G The relative ratios of exclusion to inclusion (−/+) were quantified. Mean ± SD, unpaired two-tailed *t*-test, *n* = 3 biological replicates.

H Representative PCR analysis to examine expression levels of the spliced mRNA isoform containing exon 2a of *STMN2* in SH-SY5Y cells with the indicated constructs (top panel). TDP-43 protein levels were examined by immunoblotting (bottom panel).

I Quantification of the relative levels of truncated *STMN2*. Mean ± SD, unpaired two-tailed *t*-test, *n* = 3 biological replicates.

J Quantification of the relative mRNA levels of *STMN2*. Results were normalized to expression of the gene encoding *ACTB* and were quantified by the change-in-threshold method (ΔΔCT). Mean ± SD, unpaired two-tailed *t*-test, *n* = 6 biological replicates.

Data information: *$P < 0.05$, **$P < 0.01$, ***$P < 0.001$, n.s., not significant.
Source data are available online for this figure.

hyperphosphorylation of the tau protein in AD brain, which causes neurofibrillary degeneration (Liu *et al*, 2004). Moreover, the OGA inhibitor TMG treatment blocks tau phosphorylation in rat brain (Yuzwa *et al*, 2008) and decreases tau aggregation and attenuates tauopathies in the tau transgenic mice (Yuzwa *et al*, 2012). In this study, we showed that abolishment of TDP-43 O-GlcNAcylation resulted in the loss of toxic gain-of-function of pathologies compared to the WT overexpression in *Drosophila* model, suggesting the importance of O-GlcNAcylation in regulating TDP-43 functions. Unfortunately, we failed to generate catalytic-inactive mutant of OGT overexpressed flies, which would provide a better approach to examine that the attenuated locomotion defects in TDP-43 over-expressed files arises from the O-GlcNAcylation on TDP-43. Alternatively, generating flies or mice model bearing the O-GlcNAcylation sites mutated TDP-43 would allow us to explore whether the O-GlcNAcylation on T199 and T233 of TDP-43 is necessary to prevent ALS-like symptoms.

How does TDP-43 O-GlcNAcylation block TDP-43 pathogenesis? One plausible explanation could be that TDP-43 is a RNA splicing factor which regulates multiple neuron-related mRNA splicing events. Indeed, compared to the normal role of WT TDP-43 in alternative splicing, mutations of O-GlcNAcylation sites compromised the ability of proper mRNA splicing in many target genes. It is important to dissect the mechanism underlying how the O-GlcNAcylated TDP-43 executed its appropriate splicing activity, thereby preventing aberrant neurite growth and axon regeneration. Although it is still unclear whether low levels of TDP-43 O-GlcNAcylation are associated with ALS or FTLD pathogenesis, our data overall support O-GlcNAc modification on TDP-43 is functionally connected to pre-mRNA splicing and related neuronal pathology.

In summary, we propose that O-GlcNAcylation of TDP-43 can modulate its splicing function and prevent TDP-43 proteinopathies. The dynamic glucose metabolism might be a switch to modulate TDP-43 O-GlcNAc levels and its function under some defined conditions. Previous studies have shown that elevated O-GlcNAc levels in spinal motor neurons protect age-dependent oxidative stress and improve cell survival, and decreased O-GlcNAC levels are found in the spinal cords of ALS model animals (Ludemann *et al*, 2005; Shan

et al, 2012; Hsieh *et al*, 2019). In addition, neuron-specific depletion of OGT leads to impaired mobility or progressive neurodegeneration in mice (O'Donnell *et al*, 2004). Future studies are needed to determine whether dynamic changes of TDP-43 O-GlcNAcylation are linked to neurodegenerative disorders, which may establish a clinical and therapeutic relevance of TDP-43 O-GlcNAcylation.

Materials and Methods

Cell culture and reagent treatment

HEK 293T cells (from ATCC), SH-SY5Y cells (from China Center for Type Culture Collection), and Neuro-2a cells (from ATCC) were grown in Dulbecco's modified Eagle's medium (DMEM, Gibco, #12800-017), or Minimum Essential Medium Eagle (MEM, Hyclone, # AC10249345) supplemented with 10% fetal bovine serum (FBS, Bio-one, #P30-3302) at 37°C under humidified 5% CO_2/air. DNA transfections were performed with lipofectamine 2000 (Invitrogen, #11668-019) according to manufacturer's instruction. To increase protein O-GlcNAc levels, a final concentration of 10 μM TMG (MedChemExpress HY-12588) and 50 μM PUGNAc (Sigma, A7229) were added into SH-SY5Y cells, respectively. To inhibit OGT activity, a final concentration of 10 μM OSMI-1 (Sigma, SML1621) was added. For O-GlcNAcylation assay, cells grown in 6-well culture dishes were treated with 5 mM GlcNAc (Sigma, A3286) for 24 h or treated with different doses of UDP-GlcNAc (Sigma, U4375) for 24 h. For EA treatment, cells were exposed to 60 μM EA (MedChemExpress, HY-B1640) for 24 h. Cells were harvested and lysed with buffer containing 25 mM Tris–HCl pH 7.4, 150 mM NaCl, 5% glycerol, 1% NP-40 plus protease inhibitors, then analyzed by immunoblotting using the indicated antibodies, as described below.

Plasmids construction and antibodies

TDP-43 and OGT constructs were cloned into pCS2-3xFlag vectors, and the indicated mutants were created by site-directed mutagenesis using primers listed in Table EV1. The OGA constructs were cloned

into the pCS2-3xHA vectors using *Eco*RI and *Xho*II restriction enzymes. To generate UAS-TDP-43 WT and mutant transgenics, human TDP-43 WT and mutants were cloned into the Gateway compatible pBID-UAS-G vector by LR reaction. pBID-UAS-G was constructed by cloning the Gateway cassette into the *Xho*I/*Xba*I sites of pBID-UAS. The antibodies were obtained from commercial sources: α-TDP-43 (ProteinTech, 10782-2-AP, 1:1,000 for immunoblotting; 12892-1-AP for immunoprecipitation; Abcam, ab10423, 1:500 for immunostaining), α-OGT (Santa Cruz, sc-32921, 1:1,000), α-OGA (also named MGEA5, ProteinTech, 14711-1-AP, 1:1,000), α-Flag (Sigma, F7425, 1:2,000), α-HA (Santa Cruz, sc-805, 1:3,000), α-Myc (Sigma, M4439, 1:3,000), α-O-GlcNAc (CTD 110.6) from Santa Cruz (sc-59623, 1:1,000; Sigma, MABS1254, 1:500), α-O-GlcNAc (RL2) from Abcam (ab2739, 1:1,000), α-phospho-TDP-43 409/410 (Cosmo Bio, 425-4, 1:2,000), and α-GFP (Sungen, KM8009, 1:3,000), α-GAPDH (ABclonal, AC002, 1:5,000), α-β-Actin (ProteinTech, 60008-1-Ig, 1:5,000).

Yeast transformation and spotting assays

Yeast stains used in this study are based on the *W303* background. For spotting assays, yeast cells expressing empty vector, various hTDP-43 constructs, indicated OGT constructs or both as indicated were grown overnight at 30°C in liquid media containing raffinose until they reached to mid-log phase. Cultures were normalized, serially diluted, and spotted onto synthetic solid media containing 2% glucose or 0.25% galactose plus 1.75% sucrose lacking uracil and leucine. The images were photographed after grown at 30°C after 2–3 days.

Biochemical separation of TDP-43 from cells

Cells from 6-well culture dishes were harvested and homogenized in lysis buffer (10 mM HEPES-NaOH pH 7.9, 10 mM KCl, 1.5 mM MgCl$_2$, 1% β-ME) supplemented with the protease inhibitor cocktails (Bimaker, B1401). SDS were then added into the lysates with the final concentration of 0.5% and rinsed on ice for 2 min and centrifuged at 15,000 *g* for 15 min at 4°C to deplete the soluble protein pool. The insoluble fractions were then washed by phosphate-buffered saline (PBS) and centrifuged at 15,000 *g* at 4°C for three times, or extracted in 200 μl urea buffer (7 M urea, 4% CHAPS, 30 mM Tris, pH 8.5) for 30 min at room temperature. All soluble and insoluble fractions were subsequently analyzed by Western blotting.

Immunofluorescence, immunocytochemistry, and quantification

GFP-TDP-43 and/or mCherry-OGT plasmids were transformed into yeast cells, and an Olympus BX51 microscope (Tokyo, Japan) and a Retiga 2000R CCD camera (QImaging Corporation, Canada) were used to visualize cell morphology by differential interference contrast and fluorescent microscopy. 100 × oil immersion objective was used. The aggregate foci numbers in each cell were counted, and over 100 cells of each sample from three biological replicates were quantified. HEK 293T cells were seeded on Poly-L-Lysine-coated coverslips, transfected as described above, and cultured in appropriate medium. After drug treatment, the cells were fixed in 4% paraformaldehyde (PFA) for 10 min, rinsed in PBS for 3 times,

and permeabilized once with 0.3% Triton X-100 in PBS for 10 min. Fixed cells were then blocked in 2% BSA for 30 min and incubated with specified primary antibodies for 2 h at room temperature or overnight at 4°C. Cells were washed in PBS and incubated with Alexa-488 (Dylight) or Cy3 (ProteinTech Company) conjugated secondary antibody. Nuclei were counterstained with 4′,6-diamidino-2-phenylindole (DAPI, Beyotime). Cells were analyzed using a confocal laser microscope (FV10-ASWJ). The relative aggregation foci counts were normalized to that of cells co-transfected with control vector, and > 4 fields and a minimum of 100 transfected cells in each field were used.

Protein digestion and LC-MS/MS analysis

Flag-TDP-43 was overexpressed in HEK 293T cells, and TDP-43 protein was immunoprecipitated and then separated in SDS–PAGE gel. The gel was stained with Coomassie blue, cut into slices and subjected to typical in-gel trypsin (Promega, V5071) digestion. The peptides were ejected into liquid chromatography followed by mass spectrometry (LC-MS/MS) as described previously (Liu *et al*, 2018). Briefly, the eluted peptides were analyzed with an Orbitrap Fusion mass spectrometer (Thermo Fisher Scientific, San Jose, CA) equipped with an online-electrospray ion source. Samples were detected with combination of higher-energy collisional dissociation (HCD) and electron transfer dissociation (ETD).

Mass spectra data analysis

Tandem mass spectra were searched against the hTDP-43 sequence using Peaks Studio 7.5. Cysteine carbamidomethylation (+57.021 Da) was set as the fixed modification. Serine/threonine O-GlcNAcylation (+203.079 Da), N-terminal acylation (+42.001 Da), and methionine oxidation (+15.995 Da) were set as the variable modifications. Tandem mass spectra corresponding to the putative O-GlcNAc-modified peptides and sites were verified by manual inspection of their fragmentation pattern. The O-GlcNAcylation sites were identified and manually confirmed using PEAKS studio software (Bioinformatics Solutions Inc.).

In vitro O-GlcNAcylation assay

Human TDP-43 cDNA fragment (a.a.102-269) and its mutants were ligated into bacterial pGEX6p-1 plasmid, and the plasmids were transformed into BL21 competent cells to induce protein expression at room temperature for 4–6 h. The TDP-43 fragments were purified using GST beads. Flag-tagged OGT was immunoprecipitated from HEK 293T cells by M2 Flag resins (Sigma), and the resins were incubated with the purified GST-TDP-43 fragments in the reaction buffer (100 mM Tris–HCl pH 7.6, 25 mM MgCl$_2$, 2 mM DTT), in the presence of 2 mM UDP-GlcNAc. The reactions were performed at 30°C, for 5 h with vibration. The GlcNAcylation levels of TDP-43 were analyzed by immunoblotting with an α-O-GlcNAc antibody.

Drosophila genetics

All flies were maintained at 25°C on standard media unless otherwise indicated. The WT and mutant hTDP-43 transgenes, UAS-TDP-43^{WT}, UAS-TDP-43^{T119A}, UAS-hTDP-43^{T233A}, and UAS-TDP-43^{2TA}

were integrated into the *att*P40 site on chromosome III using phiC31-mediated transgenesis (Groth *et al*, 2004). The fly strain UAS-HA-OGT was from the Bloomington Drosophila Stock Center. The GAL4 driver used in this study was elav-GAL*4* (Lin & Goodman, 1994).

Fly food supplementation

For 1 l regular sugar (RS) medium, 40 g sucrose (4%), 25 g yeast extract, 65 g corn powder, and 6 g agar powder were heated and mixed with 7 ml propionic acid and 0.25 g paraben were added into medium at 55–60°C. For high sugar (HS) medium, additional sucrose was added to reach a final concentration of 160 g/l (16%). Supplemented food was dispensed into vials and allowed to cool.

Larval crawling assays

The third instar larvae of the indicated genotypes stocks were transferred onto the surface of agar plates filled with 2% sucrose and 2% agar and allowed to acclimate. Video was recorded for 60 s of the moving tracks of each larva. During video capture, the moving larva was kept in the field of view under the microscope. At least 8 different larvae from each strain were recorded and larval locomotion data were analyzed by ImageJ and quantified using GraphPad Prism 7.0.

Locomotor assays

All experiments were performed at the same time of day to avoid variation caused by circadian rhythm. 5-day-old adult flies were tapped into glass cylinder without anesthesia. After 10-min acclimation, flies were gently tapped to the bottom of the cylinder. After using camera to record the fly crawling distance for over 60 s, the locomotion data were analyzed using GraphPad Prism 7.0. At least 40 adult flies were used for one sample. The test was repeated three times, and results were averaged. The data are the mean of three trials and are expressed as mean ± SD. Statistical comparisons were performed using one-way ANOVA followed by Tukey's multiple comparison test.

Life span assays

Adult flies were cultivated in vials with fresh food at 25°C, and flies were transferred to vials with fresh food every 3–4 days to avoid unnatural death. The number of living flies was counted every day, and the Kaplan–Meier survival curve was plotted and analyzed using GraphPad Prism 7.0, and the log-rank test was used to determine statistical significance for survival curve. At least 30 adults for each group were assayed for survival.

RNA extraction, real-time PCR, and RNA splicing assay

Total RNAs from Neuro-2a cells were extracted using TRIzol (Life Technology) according to the manufacturer's instructions. Complementary DNA was generated from the total RNA using oligo dT primers and reverse transcriptase (Thermo Scientific) as instructed by the manufacturer's instruction. Candidate TDP-43 splicing targets were examined by PCR amplification with specific primers

(Table EV1) using PCR mix (TSINGKE Company). PCR reaction products were analyzed on 2% DNA agarose gel staining with Super GelRed (Cat No. S-2001, US Everbright Inc.). Real-time PCR was performed using qPCR mix (SYBR Green, YeaSen Company) and CFX96 Real-Time PCR Detection System (Bio-Rad). *In vitro* CFTR exon 9 skipping assay was performed as described previously (Che *et al*, 2011). TDP-43 was knocked down by transfected with a synthetic siRNA in SH-SY5Y cells or stably transfected with a doxycycline-induced shRNA targeting *TDP-43*. The oligo. siRNA was synthesized by GenePharma Company (Shanghai), and siRNA targeting *TDP-43* is 5'-GGCUCAAGCAUGGA-UUCUA-3', which has been used previously (Tollervey *et al*, 2011). The shTDP-43 sequence is 5'-CCGGAGGAATCAGCGTGCATA-TATTCTCGAGAA TATATGCACGCTGATTCCTTTTTTG-3'. The intensities of different splice isoforms were quantified using ImageJ software, and the relative ratios between the isoform with exon exclusion (−) vs. the isoform with exon inclusion (+) were quantified.

RNA-EMSA

This assay was performed as described previously (Chen *et al*, 2019). Briefly, 10 μg of total cell lysate in RIPA (10 mM HEPES pH 7.3, 20 mM KCl, 1 mM MgCl$_2$, 1 mM DTT, 5% glycerol) containing RNase inhibitor (Thermo Scientific, EO0381) was mixed with 2.5 nM of biotin-labeled RNA for IL-6 intron 2 (biotin-5'-AUGC CUCCCAGCACUUGG-GAGGCAC-3') (Lee *et al*, 2015) and the 20 μl reaction mixer was incubated for 30 min at room temperature. The binding reactions were run on a 6% non-denaturing polyacrylamide gel in 0.5× TBE buffer and subjected to Nylon membrane (Thermo Scientific, prod#77016) transferring and UV crosslinking. RNA signals were detected by horseradish peroxidase-conjugated streptavidin (Beyotime, A0303).

Statistical analysis

Unless otherwise indicated, data are presented as the mean ± SD from three biological replicates, and the differences between any two groups were compared by unpaired two-tailed *t*-tests. A value of $P < 0.05$ was considered to be statistically significant. *$P < 0.05$, **$P < 0.01$, ***$P < 0.001$, ****$P < 0.0001$ and n.s. indicates "not significant".

Data availability

This study includes no data deposited in external repositories.

Expanded View for this article is available online.

Author contributions

HND and JW designed research studies; MJZ, XY, PW, CZ, MC, DZ, WX, WTH, LLJ, JW, and HND conducted experiments; XY, MJZ, PW, WX, and JW conducted *Drosophila* experiments; JS and HS acquired and analyzed MS data; WLX, XZ, ZL, HYH, YL, YanZ, YuZ, and LZ provided new reagents and samples; MJZ, XY, PW, CZ, WJS, JW, and HND analyzed data; HND and JW wrote the manuscript with the inputs from others.

Conflict of interest

The authors declare that they have no conflict of interest.

References

Arai T, Hasegawa M, Akiyama H, Ikeda K, Nonaka T, Mori H, Mann D, Tsuchiya K, Yoshida M, Hashizume Y *et al* (2006) TDP-43 is a component of ubiquitin-positive tau-negative inclusions in frontotemporal lobar degeneration and amyotrophic lateral sclerosis. *Biochem Biophys Res Commun* 351: 602 – 611

Arnold CS, Johnson GV, Cole RN, Dong DL, Lee M, Hart GW (1996) The microtubule-associated protein tau is extensively modified with O-linked N-acetylglucosamine. *J Biol Chem* 271: 28741 – 28744

Arnold ES, Ling SC, Huelga SC, Lagier-Tourenne C, Polymenidou M, Ditsworth D, Kordasiewicz HB, McAlonis-Downes M, Platoshyn O, Parone PA *et al* (2013) ALS-linked TDP-43 mutations produce aberrant RNA splicing and adult-onset motor neuron disease without aggregation or loss of nuclear TDP-43. *Proc Natl Acad Sci USA* 110: E736 – E745

Barmada SJ, Skibinski G, Korb E, Rao EJ, Wu JY, Finkbeiner S (2010) Cytoplasmic mislocalization of TDP-43 is toxic to neurons and enhanced by a mutation associated with familial amyotrophic lateral sclerosis. *J Neurosci* 30: 639 – 649

Bilen J, Bonini NM (2005) Drosophila as a model for human neurodegenerative disease. *Annu Rev Genet* 39: 153 – 171

Buratti E, Baralle FE (2001) Characterization and functional implications of the RNA binding properties of nuclear factor TDP-43, a novel splicing regulator of CFTR exon 9. *J Biol Chem* 276: 36337 – 36343

Buratti E, Baralle FE (2008) Multiple roles of TDP-43 in gene expression, splicing regulation, and human disease. *Front Biosci* 13: 867 – 878

Buratti E, Dork T, Zuccato E, Pagani F, Romano M, Baralle FE (2001) Nuclear factor TDP-43 and SR proteins promote in vitro and in vivo CFTR exon 9 skipping. *EMBO J* 20: 1774 – 1784

Che MX, Jiang YJ, Xie YY, Jiang LL, Hu HY (2011) Aggregation of the 35-kDa fragment of TDP-43 causes formation of cytoplasmic inclusions and alteration of RNA processing. *FASEB J* 25: 2344 – 2353

Chen HJ, Topp SD, Hui HS, Zacco E, Katarya M, McLoughlin C, King A, Smith BN, Troakes C, Pastore A *et al* (2019) RRM adjacent TARDBP mutations disrupt RNA binding and enhance TDP-43 proteinopathy. *Brain* 142: 3753 – 3770

Choksi DK, Roy B, Chatterjee S, Yusuff T, Bakhoum MF, Sengupta U, Ambegaokar S, Kayed R, Jackson GR (2014) TDP-43 Phosphorylation by casein kinase Iepsilon promotes oligomerization and enhances toxicity in vivo. *Hum Mol Genet* 23: 1025 – 1035

Cohen TJ, Hwang AW, Restrepo CR, Yuan CX, Trojanowski JQ, Lee VM (2015) An acetylation switch controls TDP-43 function and aggregation propensity. *Nat Commun* 6: 5845

Cohen TJ, Lee VM, Trojanowski JQ (2011) TDP-43 functions and pathogenic mechanisms implicated in TDP-43 proteinopathies. *Trends Mol Med* 17: 659 – 667

Daigle JG, Lanson Jr NA, Smith RB, Casci I, Maltare A, Monaghan J, Nichols CD, Kryndushkin D, Shewmaker F, Pandey UB (2013) RNA-binding ability of FUS regulates neurodegeneration, cytoplasmic mislocalization and incorporation into stress granules associated with FUS carrying ALS-linked mutations. *Hum Mol Genet* 22: 1193 – 1205

Estes PS, Boehringer A, Zwick R, Tang JE, Grigsby B, Zarnescu DC (2011) Wild-type and A315T mutant TDP-43 exert differential neurotoxicity in a *Drosophila* model of ALS. *Hum Mol Genet* 20: 2308 – 2321

Groth AC, Fish M, Nusse R, Calos MP (2004) Construction of transgenic *Drosophila* by using the site-specific integrase from phage phiC31. *Genetics* 166: 1775 – 1782

Hasegawa M, Arai T, Nonaka T, Kametani F, Yoshida M, Hashizume Y, Beach TG, Buratti E, Baralle F, Morita M *et al* (2008) Phosphorylated TDP-43 in frontotemporal lobar degeneration and amyotrophic lateral sclerosis. *Ann Neurol* 64: 60 – 70

Heiss WD, Szelies B, Kessler J, Herholz K (1991) Abnormalities of energy metabolism in Alzheimer's disease studied with PET. *Ann N Y Acad Sci* 640: 65 – 71

Hoyer S (2004) Glucose metabolism and insulin receptor signal transduction in Alzheimer disease. *Eur J Pharmacol* 490: 115 – 125

Hsieh YL, Su FY, Tsai LK, Huang CC, Ko YL, Su LW, Chen KY, Shih HM, Hu CM, Lee WH (2019) NPGPx-mediated adaptation to oxidative stress protects motor neurons from degeneration in aging by directly modulating O-GlcNAcase. *Cell Rep* 29: 2134 – 2143 e2137

Igaz LM, Kwong LK, Lee EB, Chen-Plotkin A, Swanson E, Unger T, Malunda J, Xu Y, Winton MJ, Trojanowski JQ *et al* (2011) Dysregulation of the ALS-associated gene TDP-43 leads to neuronal death and degeneration in mice. *J Clin Invest* 121: 726 – 738

Iguchi Y, Katsuno M, Takagi S, Ishigaki S, Niwa J, Hasegawa M, Tanaka F, Sobue G (2012) Oxidative stress induced by glutathione depletion reproduces pathological modifications of TDP-43 linked to TDP-43 proteinopathies. *Neurobiol Dis* 45: 862 – 870

Johnson BS, McCaffery JM, Lindquist S, Gitler AD (2008) A yeast TDP-43 proteinopathy model: Exploring the molecular determinants of TDP-43 aggregation and cellular toxicity. *Proc Natl Acad Sci USA* 105: 6439 – 6444

Kabashi E, Lin L, Tradewell ML, Dion PA, Bercier V, Bourgouin P, Rochefort D, Bel Hadj S, Durham HD, Vande Velde C *et al* (2010) Gain and loss of function of ALS-related mutations of TARDBP (TDP-43) cause motor deficits in vivo. *Hum Mol Genet* 19: 671 – 683

Khidekel N, Ficarro SB, Clark PM, Bryan MC, Swaney DL, Rexach JE, Sun YE, Coon JJ, Peters EC, Hsieh-Wilson LC (2007) Probing the dynamics of O-GlcNAc glycosylation in the brain using quantitative proteomics. *Nat Chem Biol* 3: 339 – 348

Klim JR, Williams LA, Limone F, Guerra San Juan I, Davis-Dusenbery BN, Mordes DA, Burberry A, Steinbaugh MJ, Gamage KK, Kirchner R *et al* (2019) ALS-implicated protein TDP-43 sustains levels of STMN2, a mediator of motor neuron growth and repair. *Nat Neurosci* 22: 167 – 179

Lee EB, Lee VM, Trojanowski JQ (2011) Gains or losses: molecular mechanisms of TDP43-mediated neurodegeneration. *Nat Rev Neurosci* 13: 38 – 50

Lee S, Lee TA, Lee E, Kang S, Park A, Kim SW, Park HJ, Yoon JH, Ha SJ, Park T *et al* (2015) Identification of a subnuclear body involved in sequence-specific cytokine RNA processing. *Nat Commun* 6: 5791

Lefebvre T, Ferreira S, Dupont-Wallois L, Bussiere T, Dupire MJ, Delacourte A, Michalski JC, Caillet-Boudin ML (2003) Evidence of a balance between

phosphorylation and O-GlcNAc glycosylation of Tau proteins—a role in nuclear localization. *Biochim Biophys Acta* 1619: 167−176

Li Y, Ray P, Rao EJ, Shi C, Guo W, Chen X, Woodruff 3rd EA, Fushimi K, Wu JY (2010) A *Drosophila* model for TDP-43 proteinopathy. *Proc Natl Acad Sci USA* 107: 3169−3174

Liachko NF, McMillan PJ, Guthrie CR, Bird TD, Leverenz JB, Kraemer BC (2013) CDC7 inhibition blocks pathological TDP-43 phosphorylation and neurodegeneration. *Ann Neurol* 74: 39−52

Lin DM, Goodman CS (1994) Ectopic and increased expression of Fasciclin II alters motoneuron growth cone guidance. *Neuron* 13: 507−523

Ling SC, Polymenidou M, Cleveland DW (2013) Converging mechanisms in ALS and FTD: disrupted RNA and protein homeostasis. *Neuron* 79: 416−438

Liu F, Iqbal K, Grundke-Iqbal I, Hart GW, Gong CX (2004) O-GlcNAcylation regulates phosphorylation of tau: a mechanism involved in Alzheimer's disease. *Proc Natl Acad Sci USA* 101: 10804−10809

Liu W, Han G, Yin Y, Jiang S, Yu G, Yang Q, Yu W, Ye X, Su Y, Yang Y *et al* (2018) AANL (Agrocybe aegerita lectin 2) is a new facile tool to probe for O-GlcNAcylation. *Glycobiology* 28: 363−373

Ludemann N, Clement A, Hans VH, Leschik J, Behl C, Brandt R (2005) O-glycosylation of the tail domain of neurofilament protein M in human neurons and in spinal cord tissue of a rat model of amyotrophic lateral sclerosis (ALS). *J Biol Chem* 280: 31648−31658

Manzo E, Lorenzini I, Barrameda D, O'Conner AG, Barrows JM, Starr A, Kovalik T, Rabichow BE, Lehmkuhl EM, Shreiner DD *et al* (2019) Glycolysis upregulation is neuroprotective as a compensatory mechanism in ALS. *eLife* 8: e45114

Melamed Z, Lopez-Erauskin J, Baughn MW, Zhang O, Drenner K, Sun Y, Freyermuth F, McMahon MA, Beccari MS, Artates JW *et al* (2019) Premature polyadenylation-mediated loss of stathmin-2 is a hallmark of TDP-43-dependent neurodegeneration. *Nat Neurosci* 22: 180−190

Neumann M, Sampathu DM, Kwong LK, Truax AC, Micsenyi MC, Chou TT, Bruce J, Schuck T, Grossman M, Clark CM *et al* (2006) Ubiquitinated TDP-43 in frontotemporal lobar degeneration and amyotrophic lateral sclerosis. *Science* 314: 130−133

O'Donnell N, Zachara NE, Hart GW, Marth JD (2004) Ogt-dependent X-chromosome-linked protein glycosylation is a requisite modification in somatic cell function and embryo viability. *Mol Cell Biol* 24: 1680−1690

Pesiridis GS, Lee VM, Trojanowski JQ (2009) Mutations in TDP-43 link glycine-rich domain functions to amyotrophic lateral sclerosis. *Hum Mol Genet* 18: R156−162

Polymenidou M, Lagier-Tourenne C, Hutt KR, Huelga SC, Moran J, Liang TY, Ling SC, Sun E, Wancewicz E, Mazur C *et al* (2011) Long pre-mRNA depletion and RNA missplicing contribute to neuronal vulnerability from loss of TDP-43. *Nat Neurosci* 14: 459−468

Shan X, Vocadlo DJ, Krieger C (2012) Reduced protein O-glycosylation in the nervous system of the mutant SOD1 transgenic mouse model of amyotrophic lateral sclerosis. *Neurosci Lett* 516: 296−301

Slawson C, Hart GW (2011) O-GlcNAc signalling: implications for cancer cell biology. *Nat Rev Cancer* 11: 678−684

Sreedharan J, Blair IP, Tripathi VB, Hu X, Vance C, Rogelj B, Ackerley S, Durnall JC, Williams KL, Buratti E *et al* (2008) TDP-43 mutations in familial and sporadic amyotrophic lateral sclerosis. *Science* 319: 1668−1672

Tollervey JR, Curk T, Rogelj B, Briese M, Cereda M, Kayikci M, Konig J, Hortobagyi T, Nishimura AL, Zupunski V *et al* (2011) Characterizing the RNA targets and position-dependent splicing regulation by TDP-43. *Nat Neurosci* 14: 452−458

Wang JW, Brent JR, Tomlinson A, Shneider NA, McCabe BD (2011) The ALS-associated proteins FUS and TDP-43 function together to affect Drosophila locomotion and life span. *J Clin Invest* 121: 4118−4126

Yuzwa SA, Macauley MS, Heinonen JE, Shan X, Dennis RJ, He Y, Whitworth GE, Stubbs KA, McEachern EJ, Davies GJ *et al* (2008) A potent mechanism-inspired O-GlcNAcase inhibitor that blocks phosphorylation of tau in vivo. *Nat Chem Biol* 4: 483−490

Yuzwa SA, Shan X, Macauley MS, Clark T, Skorobogatko Y, Vosseller K, Vocadlo DJ (2012) Increasing O-GlcNAc slows neurodegeneration and stabilizes tau against aggregation. *Nat Chem Biol* 8: 393−399

Yuzwa SA, Vocadlo DJ (2014) O-GlcNAc and neurodegeneration: biochemical mechanisms and potential roles in Alzheimer's disease and beyond. *Chem Soc Rev* 43: 6839−6858

Zhang YJ, Xu YF, Dickey CA, Buratti E, Baralle F, Bailey R, Pickering-Brown S, Dickson D, Petrucelli L (2007) Progranulin mediates caspase-dependent cleavage of TAR DNA binding protein-43. *J Neurosci* 27: 10530−10534

Zhang YJ, Xu YF, Cook C, Gendron TF, Roettges P, Link CD, Lin WL, Tong J, Castanedes-Casey M, Ash P *et al* (2009) Aberrant cleavage of TDP-43 enhances aggregation and cellular toxicity. *Proc Natl Acad Sci USA* 106: 7607−7612